

A. ANNEXES

A.1 INPUT DATA

A.1.1 Determination of Stress Intensity Correction Factors

In order to simplify the calculation, the stress intensity correction factor Y can be divided into sub-factors. In some publications, Y is given as a product of 3 or 4 factors [A.1], [A.2]. However, use of too many sub-factors lead to confusion. Bremen [A.3], and Dubois [A.4] distinguish *two* sub-factors of Y :

$$Y = F_c \cdot F_f \quad (\text{A.1})$$

F_c in Equation (A.1) is the *stress correction factor*, which accounts for the variation of stress distribution along the crack path¹. F_f in Equation (A.1) is the *geometry correction factor*, and depends on the detail and crack geometry. Methods exist which can be used to determine Y directly, without using Equation (A.1). Two different methods to determine stress intensity correction factor can be distinguished :

- *Numerical* methods :
 - The weight function method [A.5], [A.6] results in a very precise determination of the stress intensity correction factor, Y , provided that the stress intensity correction factor solutions for at least two reference crack loading cases, are known². In addition, the weight function method allows on to determine the crack opening displacement field [A.7].
 - Determination of the stress intensity factor using a *linear-elastic finite element analysis* of the cracked body [A.8]. This method allows on to the determine the stress intensity factor for very complex details and crack geometry. The disadvantage of the method is that it is time consuming.
 - Boundary collocation method [A.9].
 - Analytical methods: stress function methods, for example [A.9].
- *Experimental* methods (photoelasticity method, for example [A.8]).

Many existing solutions of Y for various crack and detail geometry are available in handbooks [A.9], [A.10], [A.11].

A.2 MODELING DETAILS

A.2.1 Indications Concerning Element Size

The objective of this section is to conduct a brief literature review of parameters which can be used to indicate the size of the elements. Lemaitre [A.12] : “ The 'size' of the volume must be sufficiently large to represent the local properties by their mean values through continuous variables. Roughly speaking : $0.1 \cdot 0.1 \cdot 0.1$ mm for metals ... “.

¹ The stress correction factor, $F_c = 1$, equals the stress distribution along the crack path is the same as the nominal stress distribution.

² A simplified weighted function method was proposed by Albrecht and Yamada [A.2]. The method requires F_f to be known. F_c is obtained by integrating the stress concentration factor distribution along the crack path. Due to its simplicity, this method is widely used.

Element size requirements can also be related to a material microstructure parameter as it is referred to by many authors. Miller and *al.* [A.13] have found that the microstructure length parameter, which relates the distance between obstacles to crack growth, is 0.1 mm for fully annealed 0.4% carbon steel. Hobson and *al.* [A.14] have found that the microstructure length parameter for medium carbon steels equals the average ferrite plate length, which was measured to be 116 μm . Kitagawa and Takahashi [A.15] define the limit between microstructure cracks and the cracks which behave according to elastic-plastic fracture mechanics rules, to be 0.1 mm for the 0.4% carbon steel. Weiss [A.16] gives the value of Neuber's microsupport constant for high strength steels: $\rho^* = 0.05$ mm. The fracture mechanics approach to fatigue crack propagation assumes the initial crack length is about $a_0 = 0.1$ mm (for example [A.3] or [A.4]).

Glinka [A.17] postulates that “the elementary material block size can be understood rather as an average geometrical and mechanical material 'inhomogeneity' from the point of view of continuum mechanics“. In order to calibrate his continuum mechanics based fatigue crack propagation model, Glinka, selected an the element size that is close to the material grain size. However, there appears to be a contradiction between the requirements of continuum mechanics (Condition 3.3) and the element size chosen by Glinka.

A.2.2 Loading of Elements at the Tip of Blunted Crack

In Chapter 3, equations to calculate the linear-elastic loading of elements at the tip of *sharp* and *blunted* cracks were developed. The linear-elastic stress at the tip of *blunted fatigue crack* with a tip radius ρ , at any value of the co-ordinate x , $\sigma_{le}(x)$, can be calculated using Equation (A.2) [A.18] :

$$\sigma_{le}(x) = \frac{K_{eff}}{\sqrt{2 \cdot \pi \cdot x}} \cdot \left(1 + \frac{\rho}{2 \cdot x} \right) \quad (\text{A.2})$$

Substituting the right side of Equation (A.2) for the $\sigma_{le}(x)$ in Equation (3.12), the right side of Equation (3.17) for the $x_{0,k}$ in Equation (3.12), and integrating Equation (3.12) leads to the formula of the loading of elements situating at the tip of the *blunted fatigue crack* :

$$\sigma_{le,j} = K_{eff} \cdot \frac{2}{\sqrt{\pi}} \cdot \frac{j \cdot \sqrt{\rho + 2 \cdot \delta \cdot (j-1)} + (1-j) \cdot \sqrt{\rho + 2 \cdot \delta \cdot j}}{\sqrt{\rho + 2 \cdot \delta \cdot (j-1)} \cdot \sqrt{\rho + 2 \cdot \delta \cdot j}} \quad (\text{A.3})$$

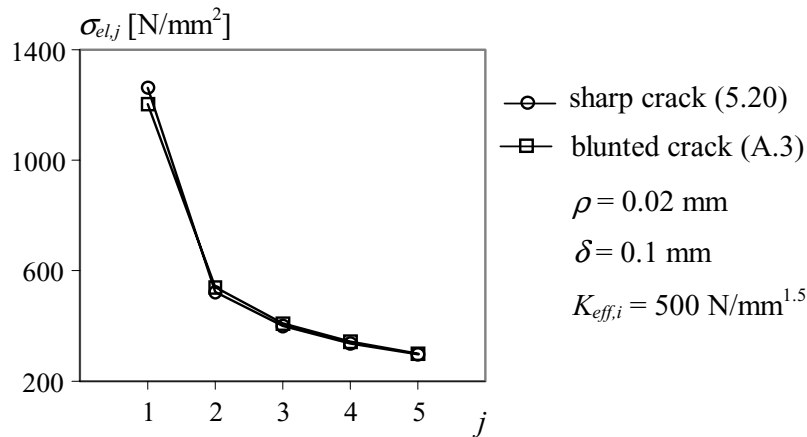


Figure A.1 : Comparison of the equations (3.18) and (A.3).

The crack tip radius ρ in Equation (A.3) can be taken equal to the material grain size [A.17]. Glinka [A.17] derived a formula similar to Equation (A.3). Figure A.1 presents the

comparison of Equations (3.18) and (A.3). The comparison shows, that for a given crack tip radius and element size, both equations lead approximately to the same loading of elements. The difference between corresponding values of the two curves of $\sigma_{le,j}$, is less than 5%.

A.2.3 Neuber's Rule

In Chapter 3 Glinka's ESED criterion was given. The aim of this clause is to present Neuber's rule which is similar to Glinka's ESED criterion. Neuber's rule was introduced by Neuber [A.19] but was generalized by Seeger and Heuler later [A.20]. Topper *et al.* [A.21] have extended Neuber's rule to cyclic loading situations.

Neuber's rule states that the sum of the non-linear strain energy density *and* the non-linear complementary strain energy density distribution in the plastic zone equals that calculated on the basis of a linear elastic stress-strain analysis : Equation (A.4) and Figure A.2.

$$U + U^* = U_{le} + U_{le}^* \quad (\text{A.4})$$

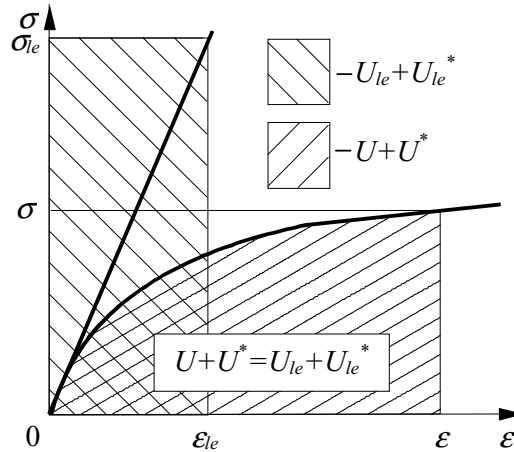


Figure A.2 : Graphical presentation of Neuber's rule.

U_{le} and U in Equation (A.4) are the linear-elastic and elastic-plastic strain energy densities, correspondingly. U_{le}^* and U^* in Equation (A.4) are the linear-elastic and elastic-plastic *complementary* strain energy densities, respectively [A.22] (see Figure A.3).

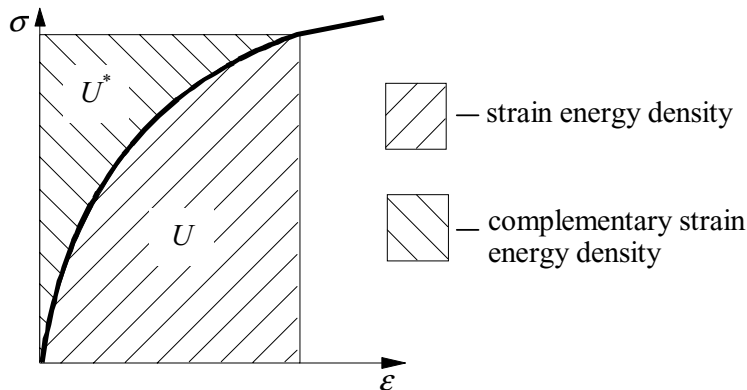


Figure A.3 : Definition of the strain energy density and the complementary strain energy density.

A.2.4 Stress-Strain Hysteresis Loops : Calculation Example

The following example is based on the algorithm given in section 3.4.1 (see Figure 3.12). If the stress-strain hysteresis loops are calculated *correctly*, then they will stabilize after the occurrence of the first absolute maximum nominal stress peak (peak $i = 3$ in Figure A.4.a). If the stress-strain hysteresis loops are calculated *incorrectly*, then the calculated hysteresis loops will not stabilize (Figure A.4). Indexes $i0$ and calculation steps for the elastic-plastic stress σ_i , and strain ε_i , for all load reversals i , in Figure A.4.a, are presented in Table A.1.

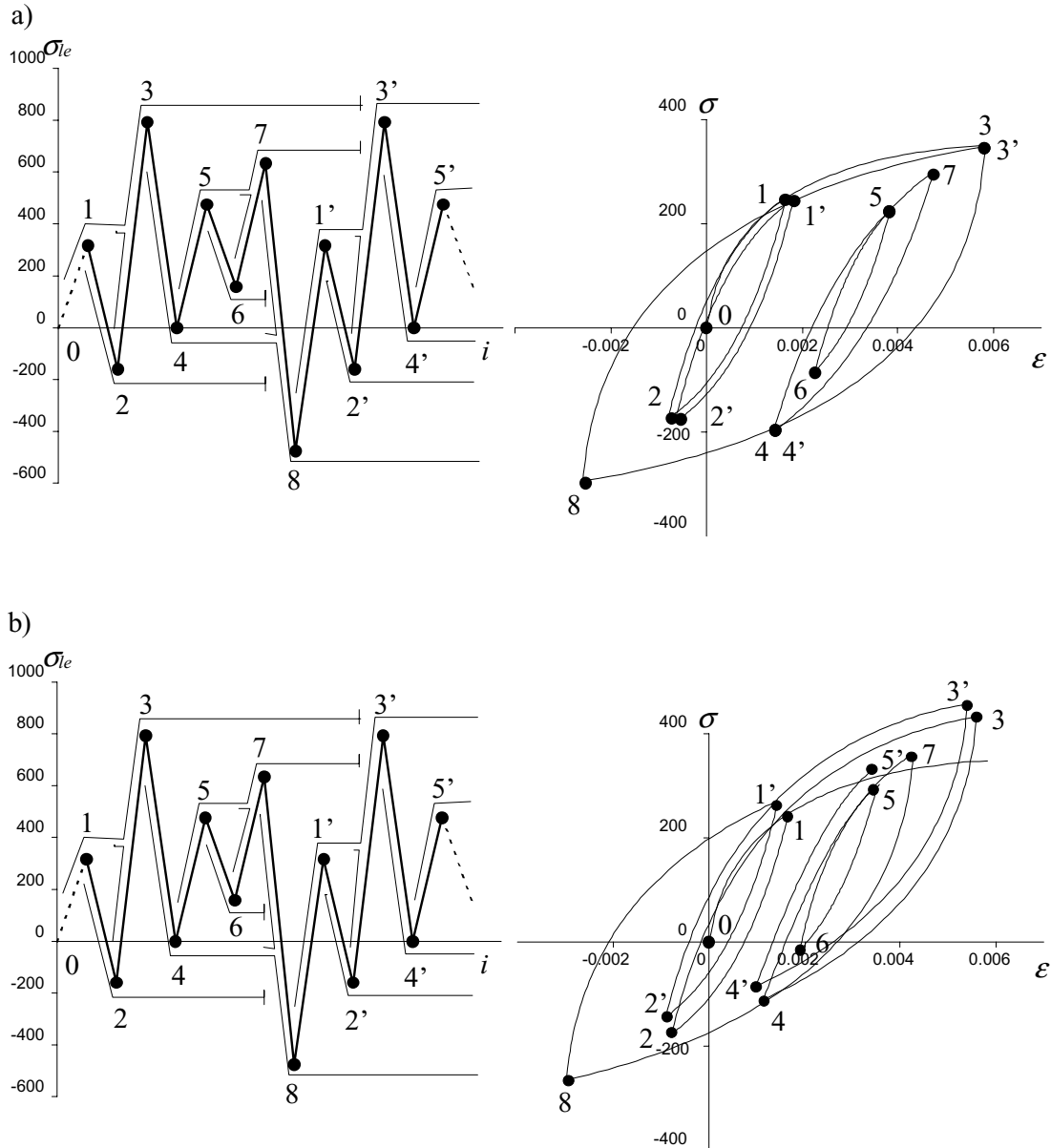


Figure A.4 : Elastic-plastic stress-strain hysteresis loops calculated as a functions of loading of element : a) stabilized, correctly calculated loops ; b) non-stabilized, incorrectly calculated loops.

i	$i0$	Calculation step in Figure 3.12
1	0	3
2	1	4
3	0	3
4	3	4
5	4	4
6	5	4
7	4	4
8	3	4
1'	8	4
2'	1'	4
3'	8	4
4'	3'	4
5'	4'	4
...

Table A.1 : Calculation of the elastic-plastic stress-strain hysteresis loops.

Figure A.5 illustrates the influence of fabrication-introduced residual stress σ_{res} on the stress-strain hysteresis loops. The linear elastic peaks of the stress history are increased or decreased dependent on the magnitude of the residual stress σ_{res} . Corresponding elastic-plastic stresses and strains differ from the stresses and strains that would have been found if they had been calculated without fabrication-introduced residual stress (compare Figure A.5 to Figure A.4.a).

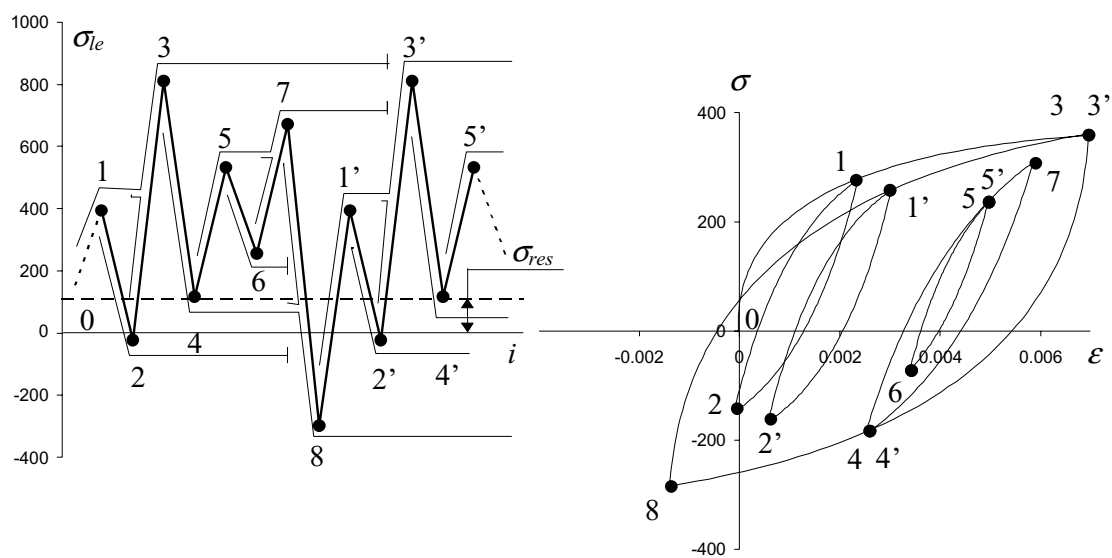


Figure A.5 : The influence of fabrication-introduced residual stresses on the stress-strain hysteresis loops.

A.2.5 Initial Crack Length

A method proposed in Clause 3.4.4 to differentiate between the crack initiation and the stable crack growth stages can be used to calculate the initial crack length, a_0 . According to Clause 3.4.4, the condition for the change of the crack propagation stage changes is :

$$\sigma_{le}(SCF) = \sigma_{le}(K_{eff}) \quad (\text{A.5})$$

where the $\sigma_{le}(SCF)$ is loading of the element calculated using the stress concentration factor (Equation 3.15) and $\sigma_{le}(K_{eff})$ is the loading of element calculated using the effective stress intensity factor (Equation 3.18). Substituting the right side of Equation (3.15) for the left side of Equation (A.5), and substituting the right side of Equation (3.18) for the right side of Equation (A.5) gives :

$$\frac{\sigma_0}{\delta} \int_{\delta^{(k-1)}}^{\delta^k} SCF(x) dx = K_{eff} \cdot \sqrt{\frac{2}{\pi \cdot \delta}} \cdot (j - \sqrt{j-1}) \quad (\text{A.6})$$

Simplifying Equation (A.6) leads to the relationship (A.7), where the initial crack length a_0 can be determined by iterating¹ :

$$\int_{a_0}^{a_0+\delta} SCF(x) dx = Y(a_0) \cdot \sqrt{2 \cdot a_0 \cdot \delta} \quad (\text{A.7})$$

It can be seen from Equation (A.7) that the initial crack length a_0 depends on the form of the stress concentration factor distribution $SCF(x)$ and the stress intensity correction factor $Y(a_0)$. Both quantities depend only on detail geometry. It can be concluded that the initial crack length a_0 is a function of detail geometry.

A.3 NORMALIZATION OF CRACK CLOSURE PARAMETERS

The objective of this section is to present the formulas used to normalize some parameters of the crack closure model (Clause 3.5.2). The crack opening stress, σ_{op} , in the crack closure model, depends on the cyclic yield stress, σ'_{ys} , and the minimum and maximum nominal stresses, $\sigma_{0,max}$, and $\sigma_{0,min}$. Normalization of the σ_{op} , σ'_{ys} , $\sigma_{0,max}$, and $\sigma_{0,min}$, results in three parameters : the effective stress ratio, R_{eff} :

$$R_{eff} = \frac{\sigma_{op}}{\sigma_{0,max}} \quad (\text{A.8})$$

the minimum and maximum nominal stress ratio, R :

$$R = \frac{\sigma_{0,min}}{\sigma_{0,max}} \quad (\text{A.9})$$

and the maximum nominal stress and cyclic yield stress ratio, R_{ys} :

$$R_{ys} = \frac{\sigma_{0,max}}{\sigma'_{ys}} \quad (\text{A.10})$$

¹ Simplification means that the effective stress intensity factor K_{eff} in Equation (A.6) is substituted with the right side of Equation (2.7) and that j is taken equal to 1 in Equation (A.6). The integration limits are expressed as a function of the initial crack length.

A.4 SOME APPLICATION ASPECTS AND DETAILS

The aim of this section is to present some aspects and details related to applications of the present study.

A.4.1 Determination of $\Delta\sigma_{0,eff}$ from $\Delta\sigma_0-N_f$ Curves

$\Delta\sigma_0-N_f$ -curves, as function of the minimum and maximum nominal stress ratio R in Figure 5.18, can be used to determine the *approximate* effective nominal stress range $\Delta\sigma_{0,eff}$. It is assumed that condition (A.11) is true.

$$\text{if } R \geq 0.5 \quad \text{then} \quad \Delta\sigma_{0,eff} = \Delta\sigma_0 \quad (\text{A.11})$$

It is also assumed that equal effective nominal stress ranges result in equal fatigue lives. Therefore, at some fixed value of cycles N_{fixed} , all the fatigue resistance curves, regardless the value of R , are loaded by the same effective stress range $\Delta\sigma_{0,eff}$:

$$\Delta\sigma_{0,eff}(N_{fixed}, R < 0.5) = \Delta\sigma_0(N_{fixed}, R = 0.5) \quad (\text{A.12})$$

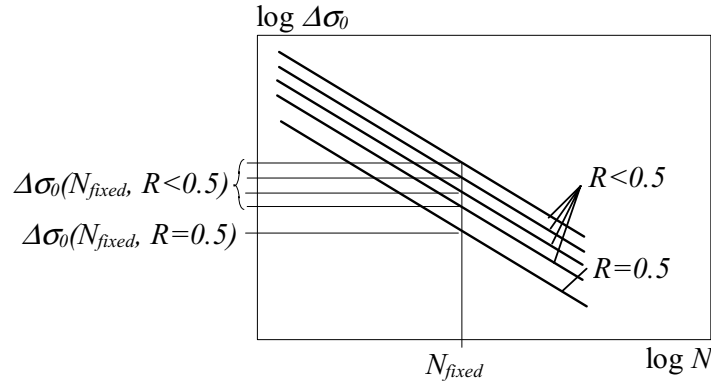


Figure A.6 : Approximate estimation of the effective stress ratio.

The symbols in the Equation (A.12) are presented in Figure A.6.

A.4.2 Determination of $\Delta\sigma_m$ from $K_{eff,max}$ and ΔK_{eff}

In this section the derivation process of Equation (6.14) is shown. Local mean stress σ_m can be written as function of local maximum stress σ_{max} and local stress range $\Delta\sigma$:

$$\sigma_m = \sigma_{max} - \frac{\Delta\sigma}{2} \quad (\text{A.13})$$

It is assumed that the local maximum stress σ_{max} at fatigue crack tip is essentially *plastic*. Using the *plastic* component of Glinka's ESED criterion (3.27) the maximum stress σ_{max} in Equation (A.13) can be expressed as a function of linear-elastic stress σ_{le} :

$$\sigma_{max} = K' \cdot \left[\frac{n'+1}{2 \cdot E \cdot K'} \right]^{\frac{n'}{n'+1}} \cdot (\sigma_{le})^{\frac{2 \cdot n'}{n'+1}} \quad (\text{A.14})$$

The linear-elastic stress σ_{le} in Equation (A.14) can be calculated using Equation (3.18). Taking $j=1$ and substituting the σ_{le} and $K_{eff,max}$ for the $\sigma_{le,j}$ and K_{eff} in Equation (3.18) leads to:

$$\sigma_{le} = K_{eff,max} \cdot \sqrt{\frac{2}{\pi \cdot \delta}} \quad (\text{A.15})$$

The substitutions made in order to obtain the local mean stress σ_m in Equation (6.14) as a function of the $K_{eff,max}$ and ΔK_{eff} , are presented in Figure A.7.

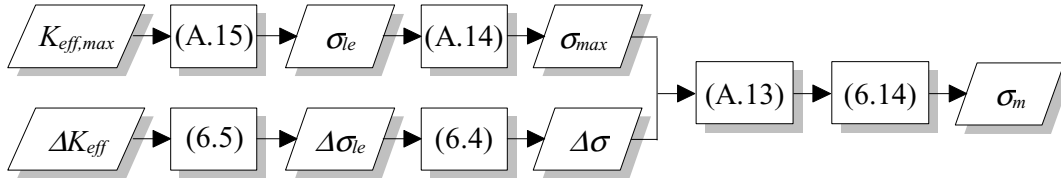


Figure A.7 : Substitutions made in order to obtain Equation (A.16) and σ_m .

A.4.3 Calculation of Variable-Amplitude Load Histories

The aim of this clause is to discuss details of calculations for 64 variable-amplitude load histories used in the example given in Clause 6.4.2. These load histories are obtained by passing the axles of 8 standard trains over linearly varying influence lines. These standard trains were taken from [A.23]. The shape of the influence line used is given in Figure A.8. Four lengths of influence lines L_{il} have been chosen for calculations : 5, 10, 15 and 20 m.

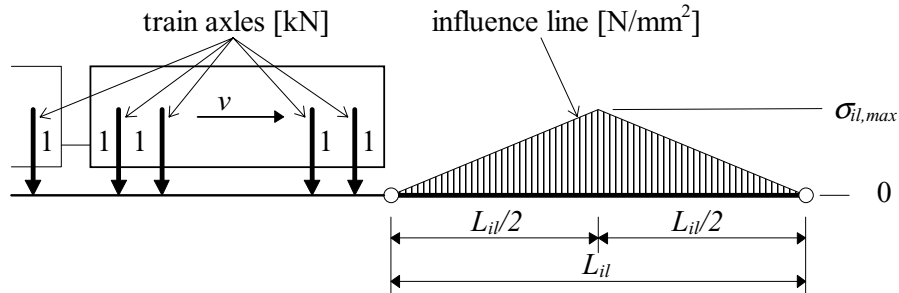


Figure A.8 : Influence line used for the generation of load histories.

The maximum value of the influence line, $\sigma_{il,max}$, is the nominal stress in $[\text{N}/\text{mm}^2]$ due to passage of *one* train axle of weight 1.0 kN over the influence line. The simulations were made using *two* values of the $\sigma_{il,max}$: 0.167 and 0.5 N/mm^2 .

Load histories obtained corresponding to the $\sigma_{il,max}=0.5 \text{ N}/\text{mm}^2$ are presented in Figure A.9. The symbols T1, T2, T3 etc. in the figure assign corresponding train types given in [A.23]. The equivalent constant-amplitude stress ranges $\Delta\sigma_e$, corresponding to variable-amplitude load histories, were calculated using the Equation 5.17 and are also presented in the same figure.

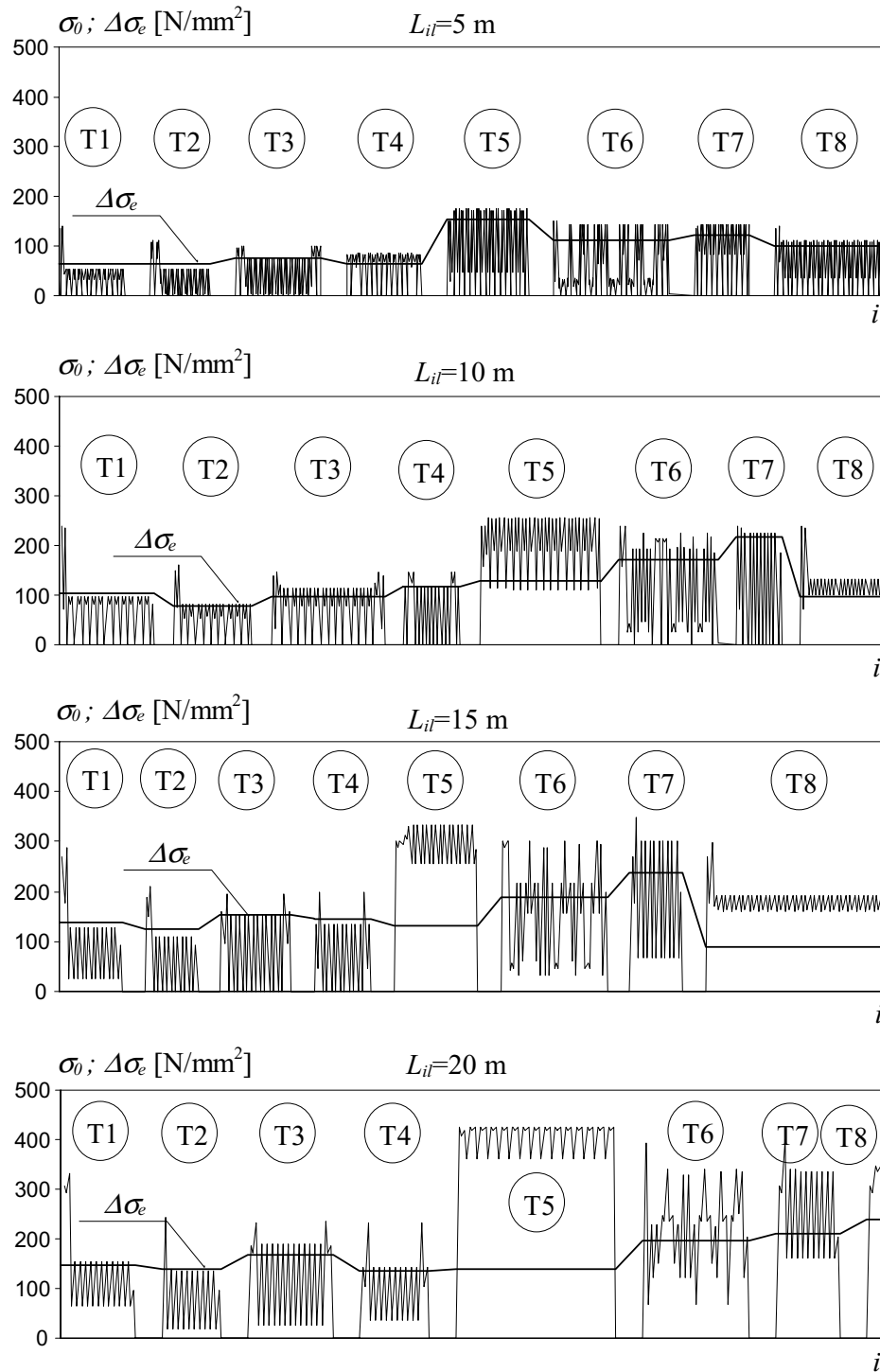


Figure A.9 : Variable-amplitude load histories obtained by standard train passage over the linear influence lines ($\sigma_{il,max}=0.5 \text{ N/mm}^2$).

